THE IMPORTANCE OF RHEOLOGY SHEAR RATE RANGE FOR DNS OF TURBULENT FLOW OF YIELD STRESS FLUIDS

Murray Rudman[1], Jagmohan Singh[1], Hugh M. Blackburn[1], Andrew Chryss[2], Lachlan J. Graham[2] and Lionel Pullum[3]

[1]*Dept. of Mech. & Aerospace Engineering, Monash University 3800 Vic., Australia*

[2]*CSIRO Minerals Resources Flagship, Clayton Vic., Australia*

[3]*Private Consultant, Olinda, Vic., Australia*

Detailed experimental measurement in non-Newtonian fine particle suspensions is difficult because they are usually opaque. Computational modelling (in particular Direct Numerical Simulation, DNS) allows great insight to be obtained into the processes occurring in turbulent flows, however most exisiting DNS of these fluids have shown significant discrepancy between experiment and simulation that is not reconciled. Here we demonstrate that accurate rheology measurement over an appropriate shear rate range is a crucial factor in reducing the discrepancy between measurement and simulation. We show this using DNS and pipe flow measurements and confirm that traditional approaches to approximating the rheology can lead to significant error. Provided rheology measurements are undertaken over a suitable range, good agreement between DNS and measurement of turbulent generalised Newtonian fluids is possible with simple rheology models. We provide a criterion for the maximum shear rate required for good answers.

KEY WORDS: Generalised Newtonian fluids (GNF), Turbulent pipe flow, computational fluid dynamics (CFD), direct numerical simulation (DNS), rheology.

1 INTRODUCTION

Many fluids in industrial applications show generalized Newtonian behaviour i.e. the fluid stress is related to the strain (or shear) rate via a non-uniform viscosity. The effective viscosity (i.e. shear stress divided by shear rate) for these fluids is often written as a function of the local shear rate. Most relevant here are fine particle suspensions that are well approximated as generalized Newtonian fluids (GNFs). They are often observed to be shear thinning, have a yield stress and can be thixotropic. Though the effective viscosity of these fluids is often very high, practical flows can occur in the transitional and turbulent regimes if the flow rates are sufficiently high or pipe diameters sufficiently large. Despite the wide applications of GNF's under turbulent flow, there have been only a few studies that attempt to develop fundamental understanding and the majority of these have been experimental (Metzner and Reed 1955, Dodge and Metzner 1959, Clapp 1961, Bogue and Metzner 1963, Park *et al.* 1989, Pinho and Whitelaw 1990, den Toonder *et al*. 1997). In most cases the primary objective was to derive a general correlation for the pipe flow friction factor.

The exact nature of the stress shear-rate relationship is characterised by choosing a mathematical model (e.g. Bingham, Herschel-Bulkley) and then fitting model parameters to the rheology data. The maximum shear rate used in shear rheology measurements is typically less than 300 s^{-1}. Although the choice of rheology model is made in order to

capture the underlying physics of a flow, the rheological parameters extracted from the fitting have little intrinsic physical basis.

The Herschel-Bulkley (HB) model is commonly used for fine particle suspensions (Heywood and Cheng, 1993, de Kretser et al., 1997):

$$\tau = \tau_Y + K\dot{\gamma}^n \qquad \Rightarrow \qquad \eta = \frac{\tau_Y}{\dot{\gamma}} + K\dot{\gamma}^{n-1} \qquad \text{Eqn 1}$$

In Eqn 1, the model parameters τ_Y, K and n are the yield stress, consistency and flow index. The shear rate is defined as the second invariant of the rate of strain tensor:

$$\dot{\gamma} = \sqrt{2\sum_{i,j} S_{ij}S_{ji}} \qquad \text{where} \qquad S_{ij} = \frac{1}{2}\left(\frac{\partial u_i}{\partial x_j} + \frac{\partial u_j}{\partial x_i}\right) \qquad \text{Eqn 2}$$

Although rheomtery is often used to obtain data for fitting, an analytical expression that relates the Herschel-Bulkley model parameters to the superficial velocity versus pressure gradient relationsip in laminar pipe flow is also often used (Chhabra and Richardson, 2008). The shear rate range over which laminar flow occurs depends critically on the fluid and pipe diameter but for laboratory experiments this is usually less than 500 s^{-1} and sometimes significantly lower. Unsurprisingly, any rheology model fitted to laminar pipe data provide good prediction of the flow rate *versus* pressure drop in the laminar region. However, the discrepancy in the prediction of turbulent friction factor using the same rheology fit can be significant. Heywood and Cheng (1993) reports discrepancy as high as 50%. Despite this, it is not uncommon to use such model fits for predicting turbulent flow. This is equivalent to extrapolating the rheology outside the range it was measured, sometimes by several orders of magnitude.

Computational fluid dynamics (CFD) modelling techniques that can be used for turbulent flow are the Reynolds-averaged Navier-Stokes (RANS), large eddy Simulation (LES) and direct numerical simulations (DNS). All require some means of estimating a local viscosity, often using a rheology model. Although results for the turbulent flow of GNFs using these numerical techniques show encouraging results (Sureskumar *et al.* (1997), Rudman *et al.* (2004), Rudman and Blackburn (2006), Guillou and Makhloufi (2007)), the most basic flow prediction (flow rate versus pressure drop, or equivalently friction factor) is usually in error. In previous DNS of power-law fluids, Rudman *et al.* (2004) found that for a given pressure gradient the superficial velocity predicted in their DNS was 25% lower than the experimentally measured value.

We believe, and seek to demonstrate, that rheology measurement and data fitting are the major causes of the discrepancy between DNS and experiment. The rationale for this hypothesis is that the local, instantaneous shear rates predicted in the DNS of Rudman *et al.* (2004) spanned many orders of magnitude and were significantly higher than shear rates over which rheology was measured and parameters estimated. Indeed Rudman *et al.* (2004) suggested that an imperfect fit over the range of shear rates encountered in turbulent flow might result in this discrepancy. The importance of rheology measurement at high shear rates has also been suggested by other researchers (Dodge and

Metzner (1959), Chhabra and Richardson (2008), Shook (2013)) when using engineering correlations. Thus the work here has broader implications than just DNS.

2 PIPE FLOW MEASUREMENTS

Pipe flow measurements were undertaken in a 14 m long, 44 mm ID loop (i.e. ≅ 300 *D*). Flow was driven by a Warman 2×1½ AH variable speed pump fed from a 400 L agitated tank. Pressure gradients in both the out and return (horizontal) lines were measured using differential pressure cells and the volumetric flow rate was measured with a magnetic flowmeter. A schematic of the rig is shown in Figure 1. The instrumentation was calibrated using a water-only flow curve compared against established values for a hydraulically smooth pipe. The agreement was very good, demonstrating that accurate readings for the Ultrez 980 are likely given the Carbopol solution requires higher pressure gradients than water.

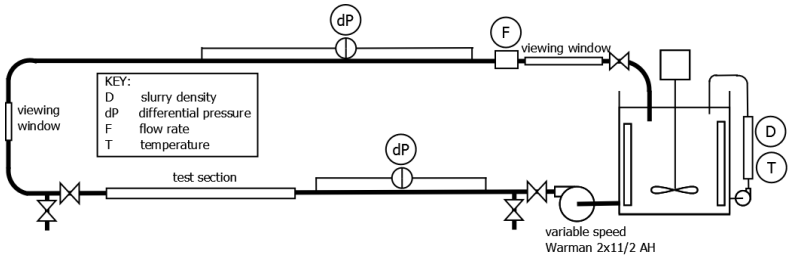

Figure 1 Schematic of the CSIRO pipe flow loop.

The Carbopol solution was made and allowed to stabilise. For each test, a series of steady flow rate conditions was established and pressure drop on both legs recorded and time-averaged. Measurements were taken for flow rates in the laminar, transitional and turbulent regimes. Pressure drop readings were sampled at 0.5 Hz for 300 s and time-averaged. Spectral analysis of the data showed only turbulence signatures indicating unintended low frequency flow phenomena did not contribute to pressure readings. Within a 95% confidence interval, the mean pressure drop reading was consistently < 1.0% of the measured value. This level of uncertainty is a similar order to that found in volumetric flow rate measurements of turbulent non-Newtonian fluids in a magnetic flow-meter Heywood and Cheng (1993).

3 RHEOLOGY MEASUREMENT

In order to cover a wide range of shear rates, rheometry was conducted in two measurement geometries: a concentric cylinder and a parallel plate (see Table 1), providing a means of confirming data where the measurements overlap (10 – 100 s^{-1}). A Haake Rheostress RS1 rheometer was used for both geometries. Temperature control was maintained via a recirculating water bath, with test temperatures matched to those of the pipe loop ± 0.1ºC. We note that Carbopol solutions can show visco-elastic behaviour at sufficiently high concentration, but at low concentrations such as used here, the fluid may be considered to be inelastic.

The concentric cylinder geometry was used to measure the lower to medium shear rate region (see Table 1). The upper range of the measurements in the concentric cylinder geometry was limited to around 100 s^{-1} due to the onset of frontal eddies at higher shear. A corrected shear rate that allows for the non-Newtonian fluid was obtained using an integration approach due to MacSporran (1986).

For the measurements in medium to high shear rate region, a parallel plate geometry creating torsional flow was used. In this geometry, the calculated rim shear stress must be corrected for non-Newtonian fluids and required the differentiation of measured instrument torque with respect to shear rate at the rim (Walters 1975). Duplicate results determined from each geometry were averaged in the region of overlapping shear rate.

Geometry	Dimensions	Shear-rate range
Concentric Cylinder	Inner-Cylinder dia.= 38mm Outer-Cylinder dia.= 41mm	0.01 - 100 s^{-1}
Parallel plate	Plate-dia.= 60mm, plate gap = 0.0002mm	10 - 15 000 s^{-1}

Table 1 Details of rheometry geometries

Laminar pipe flow measurements were also used to derive the HB model parameters. In total, five different sets of the Herschel-Bulkley model parameters were determined from the data (parameters shown in Table 2 and stress *vs* shear rate shown in Figure 2). The fit from the laminar pipe flow data (model 0) is only in reasonable agreement to the rheometry data over a narrow band of shear rate ($10 < \dot{\gamma} < 100$ s^{-1}). It deviates at low strains and is an extremely poor fit to the data at high strain rates, over-estimating it by a factor of 3 or more. Worth noting is that the maximum shear rate estimated to occur in the pipe flow measurements is around 500 s^{-1}.

Identifier	Description	τ_Y (Pa)	K	n	Re_T	Re_G
0	Laminar pipe flow	1.33	0.067	0.88	241	3 500
I	$\dot{\gamma}$ in $[0.01, 500]s^{-1}$	0.14	0.389	0.53	887	16 000
II	$\dot{\gamma}$ in $[0.01, 5000]s^{-1}$	0.52	0.177	0.65	666	11 300
III	$\dot{\gamma}$ in $[0.01, 15000]s^{-1}$	0.72	0.129	0.69	633	10 600
H	$\dot{\gamma}$ in $[1000, 15000]s^{-1}$	2.40	0.095	0.72	640	10 900

Table 2 Herschel-Bulkley rheology parameters and simulation Reynolds numbers for the 5 different rheology fitting models determined using different shear rate ranges.

The range of shear rate, $\dot{\gamma}$, used to estimate the parameters in models I, II and III increases with model number. All use data at the lowest shear rate (0.01 s^{-1}) and an upper bound (in order) of 500 s^{-1} (model I), 5 000 s^{-1} (model II), and 15 000 s^{-1} (model III). Model I corresponds to a range of shears typical used in laboratory testing (and

equivalent to the shear rates present in the laminar pipe flow measurements). As seen in Figure 2 model I also shows significant deviation from the measured data at high shear. This again demonstrates that reliable estimates of high shear rheology based on low shear measurement are likely to be problematic.

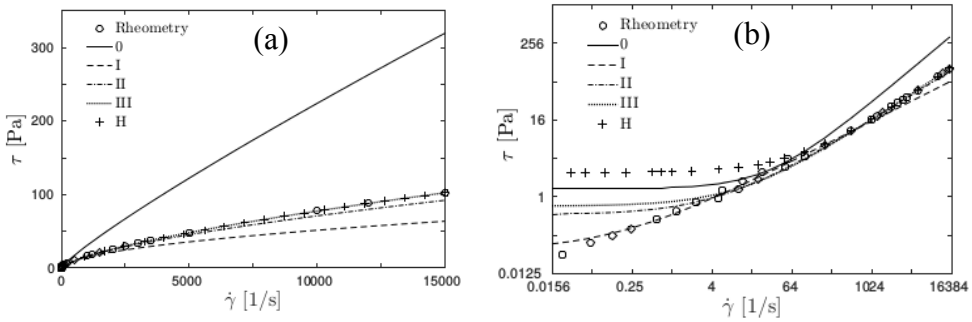

Figure 2 Stress *vs* sthear rate for the 5 different rheology fits used in this study (a) linear coordinates, (b) log-log coordinates. The measured rheology is the black circles.

Model II (upper bound 5 000 s^{-1}) was chosen based on an analysis of our DNS results that showed that local instantaneous shear rates were mostly less than 5 000 s^{-1}. Its model curve deviates slightly below the measured data at high shear rates. Model III uses the full range of measured data and deviates slightly from the measured data only at *lower* shear rates ($\dot{\gamma} < 100$ s^{-1}). A final model (model H) was determined by fitting to the measured data over the range 1 000 – 15 000 s^{-1}. It deviates significantly from the experimental data at low shear rates ($\dot{\gamma} < 250$ s^{-1}) but agrees well at high Use of this model will provide a good assessment of the importance of accurate low shear rheology.

All rheology models determined from the rheometry data (I, II, III, H) deviate from the measured data at very low shear rates (< 1 s^{-1}, not shown). This highlights the difficulty in finding a universal fit to data spanning many decades using a model with only 3 degrees of freedom. A consequence of the low shear error is that the use of any of these models to predict low speed, laminar pipe flow will provide poor results, whereas the use of model 0 will necessarily provide good results – because it is a self-referential or "closed-loop" prediction. Accurate low shear rheology measurement is difficult, however it will be seen that inadequacy in the rheology model at very low shear rates does not affect the turbulent flow predictions.

4 NUMERICAL METHOD

The numerical method used here is a branch of *semtex* (Blackburn and Sherwin 2004, Rudman and Blackburn 2006) which is a spectral element-Fourier DNS code. It solves incompressible fluid flow using the variable viscosity Navier-Stokes equations:

$$\partial u/\partial t + u\cdot\nabla u = -\nabla P + \nabla\cdot\left[\nu_{eff}\left\{\nabla u + (\nabla u)^T\right\}\right] + f \quad \text{with} \quad \nabla\cdot u = 0 \qquad \text{Eqn 3}$$

Here u is the velocity vector, P is the modified pressure i.e. pressure divided by a constant density, $\nu_{eff} = \tau/(\rho\dot{\gamma})$ is the apparent kinematic viscosity and f is the pressure

gradient. The code uses Fourier expansions in the axial direction which enforces axial periodicity. Simulations are fully unsteady and resolve all length and time scales of the unsteady flow. Simulations were run until the calculated total wall shear stress becomes statistically uniform. Time-averaged statistics were then collected for approximately twenty domain transit times.

A grid resolution and domain independence study were performed to ensure mean flow profiles and turbulence statistics did not change with mesh refinement or domain size. These were performed with rheology modell III and the final parameters chosen for the simulations run here are 16,500 grid points in a mesh cross section, 288 Fourier planes in z (giving 5.6M node points) and a periodic domain of length 4πD. Near wall mesh spacings in wall units were $\delta r^+ = 1.3$, $r\delta\theta^+ = 7$ and $\delta z^+ = 25$.

Results from the simulations are non-dimensionalised using wall units. Distance from the wall is expressed in wall units as $y^+ = yU_\tau / \nu_W$ where the friction velocity is given by $U_\tau = \sqrt{\tau_W / \rho}$ and the mean wall viscosity is determined from the pressure gradient and rheology model via

$$\nu_W = \frac{K^{1/n}\,\tau_W}{\rho\left(\tau_W - \tau_Y\right)^{1/n}} \quad \text{where} \quad \tau_W = \frac{D}{4}\frac{dP}{dz} \qquad \text{Eqn 4}$$

The Generalised Reynolds number and friction Reyniolds number are defined by:

$$\mathrm{Re}_G = \frac{UD}{\nu_W} \quad \text{and} \quad \mathrm{Re}_\tau = \frac{U_\tau D}{\nu_W} \qquad \text{Eqn 5}$$

5 RESULTS

DNS are run for two different values of axial pressure gradient: 2.33 and 2.72 kPa m^{-1}. These are the only two experimental measurements that clearly lie in the turbulent flow regime. The superficial velocity U_b measured in the experiments corresponding to these two pressure gradients was 2.71 and 2.89 m s^{-1}. Results for the higher pressure gradient (2.72 kPa m^{-1}) will be discussed first as these were run for all five rheology models (0, I, II, III, H).

5.1 Velocity and viscosity

The difference between the predicted and measured superficial velocity is shown in Figure 3 for 2.72 kPa m^{-1} as the dark grey bars. Given the discrepancy between predicted and measured rheolgy for model 0 (measured from laminar pipe flow) and model I ($\dot{\gamma}_{MAX}$ = 500 s^{-1}) poor agreement is expected and is observed in Figure 3. The superficicial velocity predicted with model 0 is almost 13% too low and with model I is about 8% too high. For the rheology models with higher shear rates, models II, III and H predict a superficial velocity that is in error by less than 2\%. This is of the order of uncertainty in the experimental measurements.

Different rheology models result in different mean axial velocity profiles as shown in Figure 4a (plotted against non-dimensional distance from the wall, y^+). Here, the flow as been arbitrarily split into four regions to assist in subsequent discussion. They are the wall region ($y^+ < 10$), buffer layer ($10 < y^+ < 30$), log layer ($30 < y^+ < 200$) and the core

region ($y^+ > 200$). In agreement with the superficial velocity results, the velocity profile for model 0 lies below the other velocity profiles and that for model I lies above. The profile for model 0 does not appear to be fully developed turbulence, and there is an absence of an obvious log-layer. The velocity profiles for the other models (II, III, H) are almost coincident.

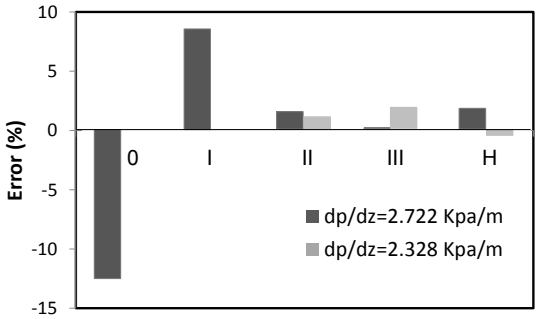

Figure 3 Error in predicted superficial velocity using DNS with different HB rheology fits.

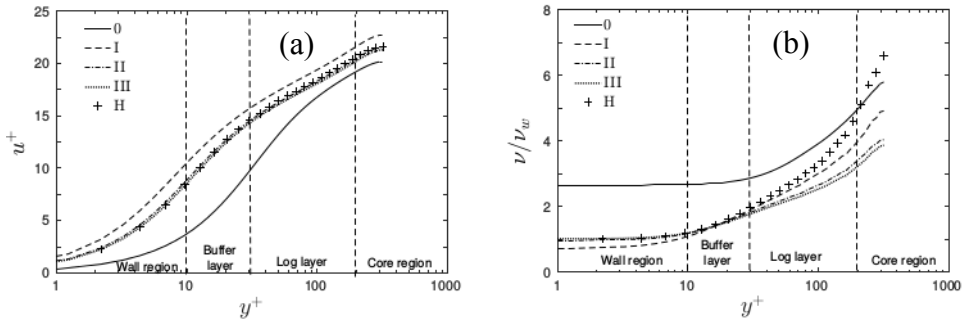

Figure 4 Profiles of (a) mean axial velocity and (b) mean viscosity for different HB models plotted in wall coordinates ($y^+ = yU_\tau / \nu_W$). The mean wall viscosity ν_W from model III is used to non-dimensionalise results in both figures.

The different rheology model fits also result in different mean viscosity profiles as shown in Figure 4b (again as a function of y^+). Model 0 deviates significantly from rheology measurement at high shear (Figure 2) and because shear at the wall is maximum, model 0 predicts a very high mean wall viscosity. The viscosity profile also lies above the other profiles for most of the pipe domain, overestimating the viscosity everywhere, not just at the wall. This explains why model 0 does not give results corresponding to fully developed turbulence. The viscosity profile for model I lies a little below that for the other models across the full radius, consistent with the prediction of a higher superficial velocity. More surpising is that the mean viscosity profiles for models II, III and H agree very well only for $y+ < 30$, which corresponds to a very small volumetric fraction of the domain (although it is the part supporting the highest shear rates). Models II and III deviate below model I in the log and core region of the domain

(where the shear rates are lower than in the near wall layers) whereas as model H deviates above for much of the flow away from the wall. This is strongly suggestive that DNS of turbulent shear thinning fluids are not significantly influenced by inaccuracies or imperfect rheology fit at low shear rates. Rheology models II, III and H were also used to simulate the turbulent flow regime with a pressure gradient of 2.33 kPa m^{-1}. Similar results were obtained and the errors in superficial flow velocity are plotted in Figure 3 as the light grey bars. The error was less than 3% in each case.

5.2 Shear rate distribution

To more clearly understand the causality in these results, it is instructive to consider the distribution of shear rates in the flow. To this end, instananeous shear rate is calculated at each grid point and a probability density function (PDF) calculated for the four different regions (wall, buffer, log and core). With the exception of model 0, the distributions do not strongly depend on the model parameters, thus only results from model III will be described in detail. The probability density function in each of the four regions describes the distribution of shear in that region and are shown in Figure 5.

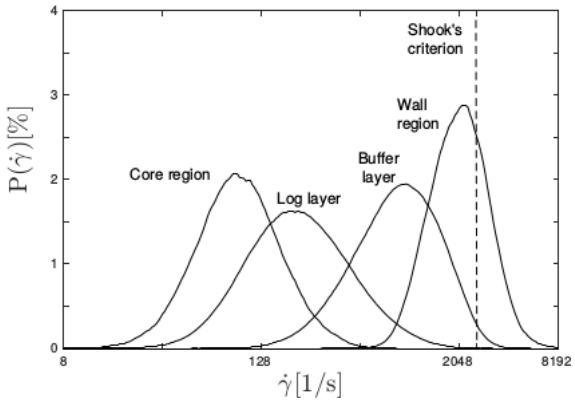

Figure 5 Probability density functions (PDF) for shear rate in each of the four flow regions (wall, buffer, log and core). Note that the shear-axis is logarithmic.

This figure clearly shows how shear rate changes with distance from the wall. The highest values occuring in the wall layer ($600 < \dot{\gamma} < 7\,000$ s^{-1}), then the buffer layer ($100 < \dot{\gamma} < 5\,000$ s^{-1}), the log layer ($20 < \dot{\gamma} < 2\,000$ s^{-1}) and core region ($\dot{\gamma} < 500$ s^{-1}). The ranges are based on a cut-off probability density of 0.01%. Most of the shear rates lie in a narrower band, e.g. only 2% of grid points in the buffer layer have $\dot{\gamma} < 500$ s^{-1}.

Already seen is that the superficial velocity estimates for model II, III and H are good and that their velocity profiles are almost coincident. However the rheology estimates for these models are only in good agreement for $\dot{\gamma} > 250$ s^{-1} (Figure 2b) and deviate from measurement at lower shear. In particular, model H over-predicts the viscosity by factors as high as four for low shear. More surprising is that nearly 50% of points in the log layer and 99% of points in the core region have $\dot{\gamma} < 250$ s^{-1}, where

model H does not accurately represent the rheology. However this error does not seem to affect the velocity estimates in any significant way. Model H gives a poor estimate of the rheology for over 50% of the total domain grid points, but gives good results for velocity. This again suggests that good low shear viscosity (for $\dot{\gamma} < 250$ s^{-1}) is less important for accurate DNS prediction than high shear viscosity. This assertion is further supported by the results for models 0 and I based on low shear measurements, but which give larger error in velocity prediction. Those models are in error primarily in the wall and buffer layers where the shear rates are high. The conclusion we draw is that because the near-wall layers dominate the dissipation, accurate rheology measurement here is absolutely essential. This corresponds to the requirement of good rheology measurement at high shear rates. Although low shear rheology does not seem important for velocity prediction, it influences the mean viscosity profile (Figure 4b). It's affect on higher order turbulence statistics and turbulence structure has not yet been quantified.

Knowing *a priori*, the range of shear rates over which rheology measurements should be undertaken is highly desirable. Shook (2013) suggested taking the rheology measurements at least up to those corresponding to the mean wall shear stress, τ_W. When expressed in terms of shear rate this is equivalent here to $\dot{\gamma}_W = 2\,600$ s^{-1}. This value is marked in Figure 5 as the vertical dashed line. There are many points in the wall region in particular where the shear rate is higher, suggesting this criterion underestimates the maximum value that encapsulates the majority of high values in the wall layer. Based on the results in Figure 5, we propose that the maximum shear rate criterion should be twice the mean wall shear rate, i.e. $\dot{\gamma}_{\max} = 2\dot{\gamma}_W$. For the HB model, this criterion can also be expressed in terms of shear stress:

$$\tau_{\max} = 2^n \tau_W + \left(1 - 2^n\right) \tau_Y \qquad \text{Eqn 6}$$

6 CONCLUSIONS

The results of this study have shown that standard methods of determining fluid rheology that use fairly low shear rates (< 500 s^{-1}) provide rheology models that can be significantly in error when used in direct numerical simulation. It appears that the dynamics of the flow in the near wall region where shear rates are the highest plays a key role in determing both the superficial velocity and the velocity profile. Thus rheology models must accurately predict the viscosity at high shear rates typical of the wall region. In turn this necessitates performing rheology measurement at these shear rates. Interestingly, it apears that accurate low shear rheology can be sacrificed and this does not adversely affect velocity predictions. We recommend that rheology measurements should be taken up to shear stresses corresponding to twice the mean wall shear rate (or given by Eqn 5), although further simulation and experiment must be done for other rheologies and Reynolds numbers to confirm this statement. This requirement is likely to present difficulties for fine particle suspensions such as mining and waste slurries, because centrifugal effects in most rheometric methodologies will tend to separate the solids. This remains an open problem.

ACKNOWLEDGEMENTS The authors thank the following companies who have sponsored aspects of this work as part of the AMIRA P1087 project "Integrated tailings management": Anglo American PLC, BASF Australia Ltd., Freeport-McMoRan Inc., Gold Fields Australasia Pty. Ltd., Outotec Pty. Ltd., Nalco-Ecolab Pty Ltd., Newmont Mining Corp., Shell Canada Energy Ltd. and Total E&P Canada Ltd.

REFERENCES

1. Blackburn, H. M. & Sherwin, S. J. 2004 Formulation of a Galerkin spectral element-Fourier method for three-dimensional incompressible flows in cylindrical geometries. Journal of Computational Physics 197 (2), 759-778.
2. Bogue, D. C. & Metzner, A. B. 1963 Velocity profiles in turbulent pipe flow. Newtonian and non-Newtonian fluids. Industrial & Engineering Chemistry Fundamentals 2 (2), 143-149.
3. Chhabra, R.P. & Richardson, J.F. 2008 Non-Newtonian Flow and Applied Rheology (Second Edition). Elsevier.
4. Clapp, R. M. 1961 Turbulent heat transfer in pseudoplastic non-Newtonian fluids. In International Development in Heat Transfer. A. S. M. E., Part 111, Sec. A., pp. 652-661.
5. Dodge, D. W. & Metzner, A. B. 1959 Turbulent flow of non-Newtonian systems. A. I. Ch. E. J. 5, 189-204.
6. Guillou, S. & Makhloufi, R. 2007 Effect of a shear-thickening rheological behaviour on the friction coefficient in a plane channel flow: A study by Direct Numerical Simulation. J. Non-Newt. Fluid Mech. 144, 73-86.
7. Heywood, N.I. & Cheng, DC-H 1993 Comparison of methods for predicting head loss in turbulent pipe flow of non-Newtonian fluids. Transactions of the Institute of Measurement and Control 6 (1), 33-45.
8. De Kretser, Ross, Scales, Peter J. & Boger, David V. 1997 Improving clay-based tailings disposal: Case study on coal tailings. AIChE Journal 43 (7), 1894-1903.
9. MacSporran, W. C. 1986 Direct numerical evaluation of shear rates in concentric cylinder viscometry. Journal of Rheology 30 (1), 125-132.
10. Metzner, A. B. & Reed, J. C. 1955 Flow of non-Newtonian fluids - correlations for laminar, transition and turbulent flow regimes. A. I. Ch. E. J. 1, 434-444.
11. Park, J.T., Mannheimer, T.A. & Grimley, T.B. 1989 Pipe flow measurements of transparent non-Newtonian slurry. Journal of Fluids Eng. 111 (3), 331-336.
12. Pinho, F. T. & Whitelaw, J. H. 1990 Flow of non-Newtonian fluids in a pipe. Journal of Non-Newtonian Mechanics 34, 129-144.
13. Rudman, M. & Blackburn, H. M. 2006 Direct numerical simulation of turbulent non-Newtonian flow using a spectral element method. Appl. Math. Mod. 30, 1229-1248.
14. Rudman, M., Blackburn, H. M., Graham, L. J. W. & Pullum, L. 2004 Turbulent pipe flow of non-Newtonian fluids. J. Non-Newt. Fluid Mech. 118 (1), 33-48.
15. Shook, C. A. & Roco, M.C. 1991 Slurry Flow: Principles and Practice. Butterworth-Heinemann.
16. Sureskumar, R., Beris, A. N. & Handler, A. H. 1997 Direct numerical simulation of the turbulent channel flow of a polymer solution. Phys. Fluids 9, 743-755.
17. den Toonder, J. M. J., Hulsen, M. A., Kuiken, G. D. C. & Nieuwstadt, F. T. M. 1997 Drag reduction by polymer additives in a turbulent pipe flow: numerical and laboratory experiments. J. Fluid Mech. 337, 193-231.
18. Walters, K. 1975 Rheometry vol. 1. London:Chapman and Hall;New York: distributed by Halstead Press.